B-spline R-matrix-with-pseudostates calculations for electron-impact excitation and ionization of carbon

Yang Wang, Oleg Zatsarinny, and Klaus Bartschat

Phys. Rev. A **87**, 012704 — Published 10 January 2013

DOI: 10.1103/PhysRevA.87.012704

B-spline R-matrix with pseudostates calculations for electron-impact excitation and ionization of carbon

Yang Wang,[1,2,*] Oleg Zatsarinny,[2,†] and Klaus Bartschat[2,‡]

[1] *Center for Theoretical Atomic and Molecular Physics, Academy of Fundamental and Interdisciplinary Sciences, Harbin Institute of Technology, Harbin, 150080, P.R. China*

[2] *Department of Physics and Astronomy, Drake University, Des Moines, Iowa, 50311, USA*

(Dated: December 27, 2012)

The *B*-spline *R*-matrix (BSR) with pseudostates method is employed to treat electron collisions with carbon atoms. Predictions for elastic scattering, excitation, and ionization are presented for incident energies between threshold and 60 eV. The structure description has been further improved compared to a previous BSR calculation by Zatsarinny *et al.* (*Phys. Rev. A* **71** (2005) 042702). This change in the structure model, together with the inclusion of a large number of pseudostates in the close-coupling expansion, has a major influence on the theoretical predictions, especially at intermediate energies, where many of the excitation cross sections are reduced significantly. Estimates for ionization cross sections are also provided.

PACS numbers: 34.80.Bm,34.80.Dp

I. INTRODUCTION

Accurate atomic data for electron collisions with carbon atoms are of importance in the modeling of many different plasmas, ranging from astrophysics (carbon is one of the most abundant elements in the universe) to the diagnostics of laboratory plasma devices, e.g., the Joint European Torus, where generalized collision radiative coefficients for fusion impurity transport modelers are required. Generally, data for neutral and single-ionized carbon, as well as molecular compounds such as CO and CO_2 are needed the most.

Despite the importance of electron collisions with neutral carbon, the available data in the literature is very sparse. As an example of a publicly available database, LXCat [1] contains just a few effective cross sections that are termed suitable for solving the two-term Boltzmann transport equation. It is not obvious, however, how reliable these cross sections actually are. To perform a serious assessment, one would undoubtedly like to have state-selective results for individual transitions, preferably experimental benchmark data, against which predictions from a number of theoretical calculations can be checked. As pointed out in our previous work on this problem [2], however, crossed-beam experimental data for excitation processes, for example, are virtually absent in the literature. Furthermore, much of the theoretical work was carried out about 25 years ago, with the notable exceptions of [2] and the work by Dunseath *et al.* [3].

The calculations reported by Zatsarinny *et al.* [2] and Dunseath *et al.* [3] were both based on the *R*-matrix method to solve the close-coupling equations. Each model coupled 28 target states and used the non-relativistic approximation, which should generally be appropriate for such a light system as carbon. An exception, however, concerns the low-energy regime up to projectile energies of about 2 eV. A strong and broad resonance below 1 eV couples differently to the three fine-structure components $(2s^2 2p^2)^3P_{0,1,2}$ of the ground-state configuration. As a result, the cross sections for elastic scattering from these three states are no longer the same, and transitions between them should also be considered. Early work on this problem was carried out by Johnson *et al.* [4].

The purpose of the present paper is to extend our previous calculations [2] further and thereby to provide an additional assessment for the likely accuracy of the available collision data. As shown in our recent work on e−Ne collisions [5, 6], coupling to the ionization continuum and, albeit to a smaller extent, the higher-lying discrete Rydberg spectrum as well as autoionizing states, can have a major effect on theoretical predictions for electron-induced transitions between the low-lying states. In the e−Ne case, the effect is most dramatic for $2p \rightarrow 3d$ single-electron transitions, even when the transition is optically allowed. The effect was originally predicted by Ballance and Griffin [7] and then confirmed in [5, 6]. Not surprisingly, it is generally even more significant for optically forbidden transitions.

Given that many important electron-induced processes in carbon also involve the $2p \rightarrow 3d$ transition, it seemed highly appropriate to carry out much larger calculations than what was possible just a few years ago. In recent years, we have extended the *B*-spline *R*-matrix (BSR) code [8] in several ways, with the most important development for the present case of interest being the ability to include a large number of pseudostates in the close-coupling expansion. As in the convergent close-coupling (CCC) [9] and standard *R*-matrix with pseudostates (RMPS) [10] approaches, these states are of finite

* Electronic Address: yangwang0624@yahoo.cn
† Electronic Address: oleg.zatsarinny@drake.edu
‡ Electronic Address: klaus.bartschat@drake.edu

range and hence represent discrete-level approximations of the high-lying Rydberg spectrum and the ionization continuum. While the coupling to these infinite manifolds cannot be accounted for exactly, the pseudostates provide a sufficiently accurate representation of the basic effect, and as an additional benefit they even allow for the calculation of ionization processes. More recent examples using the BSR code for ionization and even ionization with simultaneous excitation of helium can be found in [11, 12].

The particular advantages of our BSR implementation are: i) While the current CCC program is limited to the treatment of the valence electron(s) in quasi-one and quasi-two electron systems, the BSR suite of codes is a general package that can be applied to complex open-shell targets. ii) Compared to the well-known and frequently-used Belfast suite of R-matrix codes [13, 14], the BSR approach allows for the use of nonorthogonal orbital sets. These orbitals provide a vastly increased flexibility in the target description. Although the price to pay is a significant increase in the complexity of setting up the hamiltonian matrix and, consequently, the computational resources required, the reward of a much improved target description has in many cases been well worth the effort.

This paper is organized as follows. We begin in Sec. II by summarizing the most important changes compared to our previous work on this problem [2] for both the structure and the collision parts. This is followed in Sec. III with a presentation and discussion of our present results, in comparison with those from previous calculations and, in rare cases, experimental data. Besides elastic momentum transfer cross sections and results for state-selective excitation processes as well as electron-impact ionization, we will also lump the results in a form that might be useful for plasma applications. In particular, we will include elastic scattering, the sum of all inelastic excitations, superelastic deexcitation (in case the initial state is not the ground state), and ionization to form the "grand total cross section". Finally, we will present results from a semirelativistic Breit-Pauli model for transitions between the three states in the $(2s^22p^2)^3P_{0,1,2}$ manifold. We finish with a brief summary and conclusions in Sec. IV.

II. COMPUTATIONAL DETAILS

A. Structure calculations

The target states of carbon in the present calculations were generated by combining the multi-configuration Hartree-Fock (MCHF) and the B-spline box-based close-coupling methods [15]. Specifically, the structure of the multi-channel target expansion was chosen as

$$\begin{aligned}\Phi(2s^22pnl, LS) = &\sum_{nl} \left\{\phi(2s^22p)P(nl)\right\}^{LS} \\ &+ \sum_{nl,L'S'} \left\{\phi(2s2p^2, L'S')P(nl)\right\}^{LS} \\ &+ a\varphi(2s^22p^2)^1S + b\varphi(2s2p^3)^{LS}. \quad (1)\end{aligned}$$

Here $P(nl)$ denotes the orbital of the outer valence electron, while the ϕ and φ functions represent the configuration interaction (CI) expansions of the corresponding ionic or specific atomic states, respectively. These expansions were generated in separate MCHF calculations for each state using the MCHF program [16].

The expansion (1) can be considered a model for the entire $2s^22pnl$ and $2s2p^2nl$ Rydberg series of bound and autoionizing states in neutral carbon, including the continuum pseudostates lying above the ionization limit. The expansion can also provide a good approximation for the three states $(^3P, ^1S, ^1S)$ with the ground-state configuration $2s^22p^2$, as well as for the core-excited states $(2s2p^3)^{LS}$. Alternatively, we can choose to employ separate CI expansions for these states by directly including relaxation effects via state-specific one-electron orbitals. The latter path is usually taken in relatively small close-coupling expansions, often with only discrete states included.

The inner-core (short-range) correlation is accounted for through the CI expansion of the $2s^22p$ and $2s2p^2$ ionic states. These expansions include all single and double excitations from the $2s$ and $2p$ orbitals to the $3l$, $4l$ and $5l$ $(l = 0 - 3)$ correlated orbitals. These orbitals were generated for each state separately. To keep the final expansions for the atomic states to a reasonable size, all CI expansions were restricted by dropping contributions with coefficients whose magnitude was less than the cut-off parameter of 0.02. The resulting ionization potentials for all ionic states agreed with experiment [17] to within 0.2 eV.

The unknown functions $P(nl)$ for the outer valence electron were expanded in a B-spline basis, and the corresponding equations were solved subject to the condition that the orbitals vanish at the boundary. The B-spline coefficients for the valence electron orbitals $P(nl)$, along with the coefficient a and b for the perturbers, were obtained by diagonalizing the atomic Hamiltonian in the nonrelativistic LS-approximation. Since the B-spline bound-state close-coupling calculations generate different nonorthogonal sets of orbitals for each atomic state, their subsequent use is somewhat complicated. Our configuration expansions for the atomic target states contained at most 100 configurations for each state. These could still be used in the subsequent large-scale collision calculations with our currently available computational resources.

Table I shows a comparison between the calculated spectrum of carbon and the values of the multiplets listed in the NIST Atomic Levels and Spectra database [17].

TABLE I. Excitation energies (in eV) for the spectroscopic target states. The results are compared with energy splittings listed by NIST [17] and those obtained in our earlier BSR calculation [2].

	State	Term	[2]	Present	NIST [17]
1	$2s^22p^2$	^3P	0.000	0.000	0.000
2	$2s^22p^2$	^1D	1.353	1.302	1.260
3	$2s^22p^2$	^1S	2.833	2.629	2.680
4	$2s2p^3$	$^5S^o$	4.069	3.963	4.179
5	$2s^22p3s$	$^3P^o$	7.488	7.527	7.481
6	$2s^22p3s$	$^1P^o$	7.727	7.750	7.680
7	$2s2p^3$	$^3D^o$	8.082	8.004	7.942
8	$2s^22p3p$	^1P	8.528	8.534	8.534
9	$2s^22p3p$	^3D	8.647	8.649	8.642
10	$2s^22p3p$	^3S	8.737	8.775	8.767
11	$2s^22p3p$	^3P	8.822	8.857	8.845
12	$2s^22p3p$	^1D	9.012	9.014	8.998
13	$2s^22p3p$	^1S	9.256	9.172	9.168
14	$2s2p^3$	$^3P^o$	9.504	9.379	9.326
15	$2s^22p3d$	$^1D^o$	9.647	9.614	9.627
16	$2s^22p4s$	$^3P^o$	9.708	9.673	9.683
17	$2s^22p3d$	$^3F^o$	9.729	9.685	9.695
18	$2s^22p3d$	$^3D^o$	9.731	9.687	9.705
19	$2s^22p4s$	$^1P^o$	9.708	9.705	9.709
20	$2s^22p3d$	$^1F^o$	9.759	9.716	9.732
21	$2s^22p3d$	$^1P^o$	9.782	9.748	9.758
22	$2s^22p3d$	$^3P^o$	9.983	9.840	9.830
23	$2s2p^3$	$^1D^o$	12.984	12.968	
24	$2s2p^3$	$^3S^o$	13.273	13.073	13.114
25	$2s2p^3$	$^1P^o$	14.949	15.401	
26	$2p^4$	^3P	19.986		
27	$2p^4$	^1D	20.877		
28	$2p^4$	^1S	24.389		

The overall agreement between our results and the latter tables is satisfactory, with the deviations in the energy splitting being generally less than 0.1 eV for most states. The maximum discrepancy in the present model is 0.216 eV for the excitation threshold of the $(2s2p^3)^5S^o$ state. We believe that the current structure description is superior to that generated by Dunseath *et al.* [3], where the theoretical excitation thresholds differed by 1 eV or more for most states, and also our own previous work [2], to which we refer for a more detailed discussion of this aspect. Note, for example, that the current model predicts the correct energy sequence of all states listed. As seen from Tab. I of [2], this was not entirely the case in the previous work, where the $(2s^22p3d)^3F^o$ state lay above $(2s^22p4s)^1P^o$.

Of special interest for the discussion below are the states with principal configuration $2s2p^3$. As seen from Tab. I, the possible LS-terms for this configuration are $^5S^o$, $^3D^o$, $^3P^o$, $^1D^o$, $^3S^o$, and $^1P^o$. The first three are true bound states while the next three lie above the ionization threshold for the $(2s^22p)^2P^o$ ionic ground state around 11.3 eV. In numerical calculations like ours, these states will appear as quasi-discrete states in the continuum, and one needs to consider what will happen when they are excited in the primary collision process. As also seen from Tab. I, the three states lie below the first excitation threshold (5.3 eV) of C^+ [17], which corresponds to 16.8 eV in the table. An autoionizing decay is thus only possible to the ionic ground state.

While the $(2s2p^3)^1D^o$ and $^1P^o$ states will autoionize quickly, angular momentum and parity conservation strictly prohibits autoionization of the $(2s2p^3)^3S^o$ state in any nonrelativistic model. Autoionization will still occur in reality, for example, due to relativistic and correlation effects. Even though these effects are likely small in the particular case of the $(2s2p^3)^3S^o$ state in neutral carbon, they may nevertheless be able to compete with the generally much slower process of optical decay. To properly estimate the ionization cross section discussed below, therefore, it is important to know the branching ratio between these processes.

In order to make an estimate for this branching ratio, we performed a semirelativistic Breit-Pauli calculation for photoionization of carbon, based on the same expansion (1) as for the bound-state problem, and looked for a resonance in the channel with total electronic angular momentum $J = 1$ and odd parity near the position of the $(2s2p^3)^3S^o$ state. We indeed found such a feature, with a very small width corresponding to a decay rate of 1.5×10^9/s. Our oscillator strength for the $(2s2p^3)^3S^o - (2s^22p^2)^3P$ transition (c.f. Tab. II), on the other hand, yields an optical decay rate of 3.5×10^9/s. Consequently, we estimate a branching ratio of 30% autoionization and 70% optical decay for the $(2s2p^3)^3S^o$ state.

Another assessment of the quality of our target description can be made by comparing the results for the oscillator strengths of various transitions with experimental data and other theoretical predictions. Such a comparison is given in Tab. II with the NIST recommended values [19]. In most cases, we see good agreement between our results and the values recommended by NIST, bearing in mind that the numbers involving the $2s2p^3$ states are actually from another R-matrix calculation [18]. The oscillator strengths are very important to obtain reliable absolute values for cross sections and, ultimately, rate coefficients. Although the $(2s2p^3)^1D^o$ and $(2s2p^3)^1P^o$ states will quickly decay by autoionization, we list the dominant radiative transitions involving these states. They are important in estimating the excitation of these states in the first step, since these excitations will ultimately contribute to the observed ionization signal.

B. Scattering calculations

Our close-coupling expansion includes 696 states of carbon, with 51 states representing the bound spectrum and the remaining 645 the target continuum and core-excited autoionizing states. We included all singlet and

TABLE II. Oscillator strengths in C.

Lower level	Upper level	[2]	Present	NIST [19]
$2s^2 2p^2\,{}^3P$	$2s^2 2p3s\,{}^3P^o$	0.133	0.143	0.140
	$2s2p^3\,{}^3D^o$	0.107	0.073	0.072
	$2s2p^3\,{}^3P^o$	0.055	0.056	0.063
	$2s^2 2p4s\,{}^3P^o$	0.009	0.027	0.021
	$2s^2 2p3d\,{}^3D^o$	0.107	0.096	0.094
	$2s^2 2p3d\,{}^3P^o$	0.098	0.037	0.040
	$2s2p^3\,{}^3S$	0.134	0.156	0.152
$2s^2 2p^2\,{}^1D$	$2s^2 2p3s\,{}^1P^o$	0.118	0.103	0.118
	$2s^2 2p3d\,{}^1D^o$	0.013	0.012	0.013
	$2s^2 2p4s\,{}^1P^o$	0.004	0.007	0.011
	$2s^2 2p3d\,{}^1F^o$	0.118	0.080	0.085
	$2s^2 2p3d\,{}^1P^o$	0.011	0.011	0.009
	$2s2p^3\,{}^1D^o$	0.396	0.224	
	$2s2p^3\,{}^1P^o$	0.257	0.155	
$2s^2 2p^2\,{}^1S$	$2s^2 2p3s\,{}^1P^o$	0.098	0.090	0.094
	$2s^2 2p4s\,{}^1P^o$	0.004	0.011	0.005
	$2s^2 2p3d\,{}^1P^o$	0.196	0.116	0.125
	$2s2p^3\,{}^1P^o$	0.458	0.124	

triplet target states with total electronic angular momentum $L = 0 - 3$, plus the core-excited quintet state $(2s2p^3)\,{}^5S^o$. The continuum pseudostates in the present calculations cover the energy region up to 25 eV above the ionization limit. This model will be referred to as BSR-696 below. As a check for the sensitivity of the results regarding coupling to the high-lying Rydberg states as well as the ionization continuum, we also performed a 25-state calculation (labeled BSR-25) with the same target description for these states as in the BSR-696 model.

The close-coupling equations were solved by means of the R-matrix method, using a parallelized version of the BSR complex [8]. The distinctive feature of the method is the use of B-splines as a universal basis to represent the scattering orbitals in the inner region of $r \le a$. Hence, the R-matrix expansion in this region takes the form

$$\Psi_k(x_1,\ldots,x_{N+1}) = \mathcal{A}\sum_{ij}\bar{\Phi}_i(x_1,\ldots,x_N;\hat{\mathbf{r}}_{N+1}\sigma_{N+1})\, r_{N+1}^{-1}\, B_j(r_{N+1})\, a_{ijk} + \sum_i \chi_i(x_1,\ldots,x_{N+1})\, b_{ik}. \qquad (2)$$

Here the $\bar{\Phi}_i$ denote the channel functions constructed from the N-electron target states and the angular and spin coordinates of the projectile, while the splines $B_j(r)$ represent the radial part of the continuum orbitals. The χ_i are additional $(N+1)$-electron bound states. In standard R-matrix calculations [20], the latter are included one configuration at a time to ensure completeness of the total trial wave function and to compensate for orthogonality constraints imposed on the continuum orbitals. The use of nonorthogonal one-electron radial functions in the BSR method, on the other hand, allows us to avoid these configurations for compensating orthogonality restrictions.

In the present calculations, the bound channels were only used for a more accurate description of the $(2s^2 2p^3)^2 D^o$ and $^2P^o$ negative-ion states. These states are located very close to the ground state of carbon, and hence their position is very sensitive to the balance of correlation corrections in the N-electron target and the $(N+1)$-electron scattering functions. To maintain this balance, the multi-configuration expansions for the $(2s^2 2p^3)$ states were obtained in the same approximation as for the carbon target states. We included all single and double excitations from the $2s$ and $2p$ orbitals to the $3l$, $4l$ and $5l$ ($l = 0 - 3$) correlated orbitals and used the same cut-off parameter of 0.02.

The R-matrix radius was set to $30\,a_0$, where $a_0 = 0.529 \times 10^{-10}\,\mathrm{m}$ is the Bohr radius. We employed 83 B-splines of order 8 to span this radial range using a semi-exponential knot grid. The maximum interval in this grid is $0.65\,a_0$. This is sufficient to cover electron scattering energies up to 150 eV. The BSR-696 collision model contained up to 1,543 scattering channels, leading to generalized eigenvalue problems with matrix dimensions up to 120,000 in the B-spline basis. We calculated partial waves for total orbital angular momenta $L \le 20$ numerically and then used a top-up procedure to estimate the contribution to the cross sections from even higher L values. The calculation for the external region was performed using the STGF program [21].

III. RESULTS

A. Momentum transfer cross sections

Figure 1 shows the angle-integrated momentum transfer cross section for elastic electron scattering from carbon in the three states with the ground-state configuration $2s^2 2p^2$. Except for the low-energy regime, the results exhibit a smooth behavior as a function of energy and show little dependence on the actual angular-momentum coupling scheme. At an incident electron energy around 0.5 eV, however, the ^3P predictions exhibit a strong maximum, while the results for the other two states are still small. In the inset, we also show the "effective" cross sections that were collected by Morgan for the purpose of solving the Boltzmann transport equation in plasmas. These numbers are currently stored in the LXCat database [1]. They are generally higher than those predicted in the BSR-696 model for the individual states. The maximum, however, fits well with our results. Also, depending on the plasma temperature, more than just the ^3P ground state could contribute to the effective cross section, and hence one might qualitatively expect to see the above comparison.

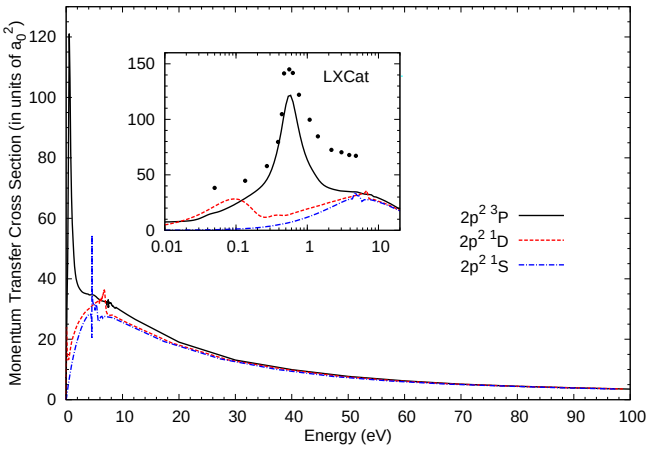

FIG. 1. (Color online) Angle-integrated momentum transfer cross section for elastic electron scattering from carbon in the $(2s^2 2p^2)^3P$, ^1D, and ^1S states, as predicted in our non-relativistic BSR-696 model. The inset shows the low-energy regime in more detail, and we also include the data points (solid circles) currently stored in the LXCat database [1].

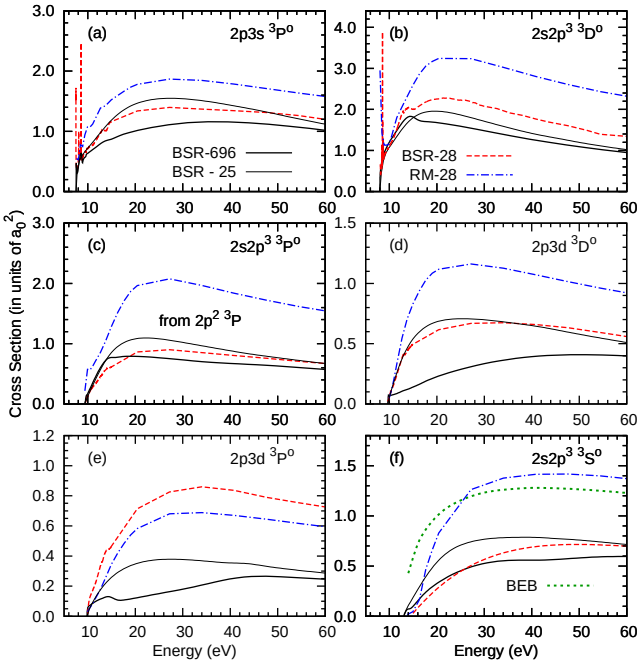

FIG. 2. (Color online) Cross sections, as a function of collision energy, for electron-impact excitation of the most important transitions from the $(2s^2 2p^2)^3P$ ground state of carbon. The final states are listed in the various panels. The present BSR-696 and BSR-25 results are compared with those from a previous standard R-matrix calculation by Dunseath *et al.* [3] and an earlier BSR calculation by Zatsarinny *et al.* [2]. Both of the latter included 28 states in the close-coupling expansion. Also shown are the BEB-scaled results of Kim and Desclaux [22] for excitation of the $(2s2p^3)^3S^o$ state.

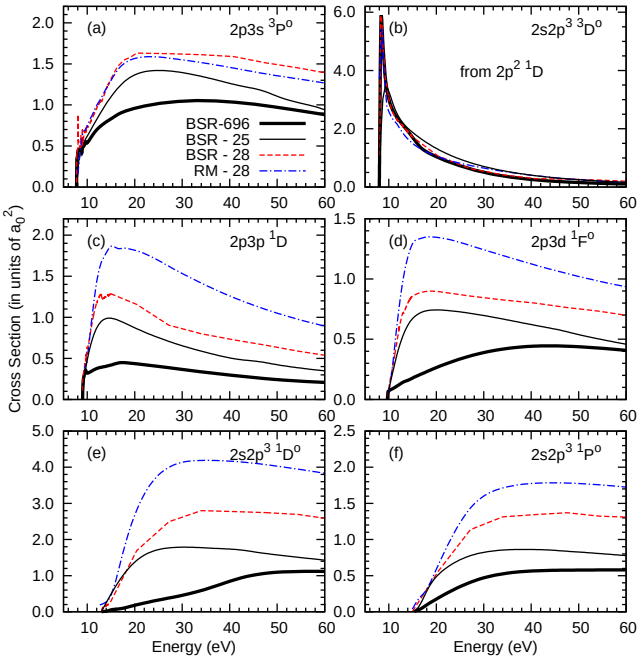

FIG. 3. (Color online) Cross sections, as a function of collision energy, for electron-impact excitation of the most important transitions from the $(2s^2 2p^2)^1D$ metastable state of carbon. The final states are listed in the various panels. The present BSR-696 and BSR-25 results are compared with those from a previous standard R-matrix calculation by Dunseath *et al.* [3] and an earlier BSR calculation by Zatsarinny *et al.* [2]. Both of the latter included 28 states in the close-coupling expansion.

B. Excitation and ionization cross sections

Cross sections as a function of energy for the most important transitions from the ground and metastable states are presented in Figs. 2-4, in comparison with the results presented by Dunseath *et al.* [3] and also our previous BSR calculations [2]. Both of the latter were 28-state close-coupling models, and hence the differences seen between the predictions from these two models are essentially due to differences in the target description, as discussed in [2]. An interesting special case is the excitation cross section of the autoionizing $(2s2p^3)^3S^o$ state. In addition to the other three calculations, we also show the semi-empirical f-scaled Binary Encounter Bethe (BEB) predictions of Kim and Desclaux [22] in Fig. 2(f). The BEB cross section increases rapidly from threshold with increasing projectile energy, and it is generally about $1\,a_0^2$ larger than the BSR-696 (and also the previous BSR-28) results. Interestingly, the BEB numbers agree much better with the standard R-matrix results [3] than with the present calculations. Note, however, that the oscillator strength in the RM-28 model is about a factor of 2 larger than the NIST-recommended value (c.f. Table II of [2]). While we recall that the latter, like our value, originates from a bound-state close-coupling calculation [18] and

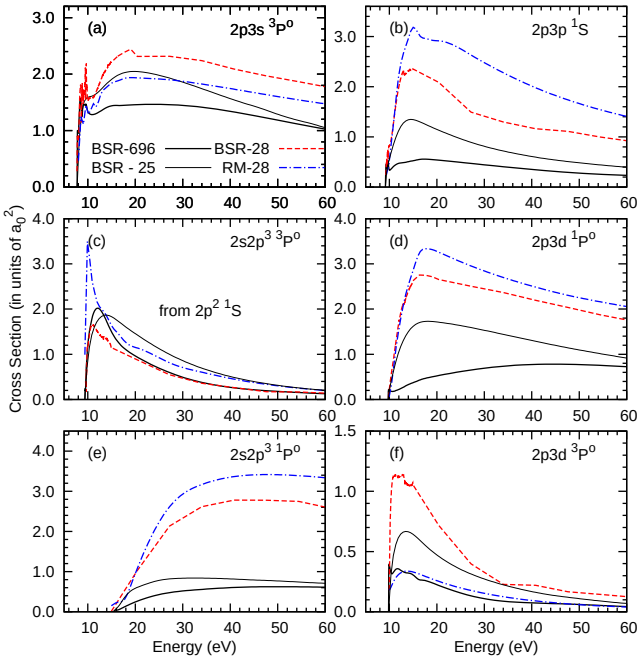

FIG. 4. (Color online) Cross sections, as a function of collision energy, for electron-impact excitation of the most important transitions from the $(2s^2 2p^2)^1S$ metastable state of carbon. The final states are listed in the various panels. The present BSR-696 and BSR-25 results are compared with those from a previous standard R-matrix calculation by Dunseath *et al.* [3] and an earlier BSR calculation by Zatsarinny *et al.* [2]. Both of the latter included 28 states in the close-coupling expansion.

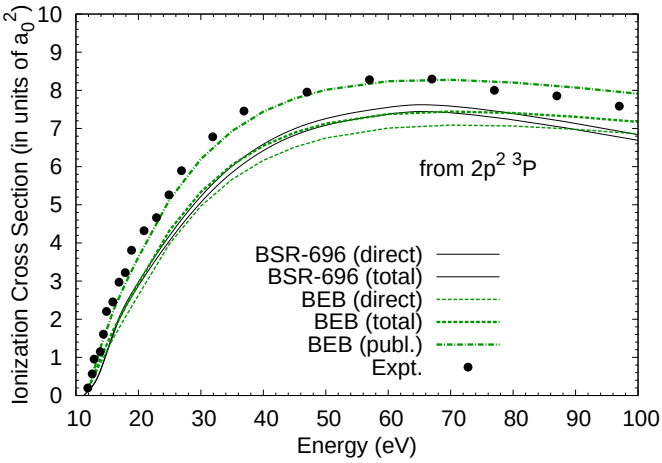

FIG. 5. (Color online) Angle-integrated cross section for electron impact ionization of carbon from the $(2s^2 2p^2)^3P$ ground state. The present BSR-696 results are compared with the BEB predictions of Kim and Desclaux [22] for both direct ionization (thinner lines) and after adding 30% of the excitation cross section for the $(2s2p^3)^3S^o$ state (thicker lines). Also shown are the experimental data of Brook *et al.* [23] and the published total BEB results (dash-dotted line). See text for details.

hence has not been validated by experiment, some doubts regarding the accuracy of both the BEB and the RM-28 predictions seem justified.

Let us first concentrate on the differences between the present BSR-696 and the previous BSR-28 results. These can be due to both differences in the structure description (see Tabs. I and II) and the collision model itself. Starting with the former, we note that the cross section for dipole-allowed transitions is closely related to the oscillator strength, and hence the difference in the absolute values for these transitions, especially at the higher energies, should follow the trends in the oscillator strengths (c.f. Tab. II). We note, however, very significant additional changes that are caused by the increased number of coupled channels. Coupling more channels generally decreases the theoretical cross sections for discrete excitation, an effect that has been seen in many other collision systems as well. (Recent examples include our BSR calculations for e−Ne collisions [5, 6].) Furthermore, sometimes the energy dependence changes as well, often by flattening out near-threshold maxima and moving them to higher collision energies. In some cases we see reductions by factors as large as 5 or even more between the BSR-696 and BSR-28 predictions, thus indicating a very strong dependence of the results on the details of the model.

In order to further test the sensitivity of our predictions, we decided to carry out a new BSR-25 calculation, in which the lowest 25 target states are identical to those in the BSR-696 model. Any differences between the predictions from these two models are then solely due to the additional channel coupling in the BSR-696 calculation. Looking at the respective results, there is no doubt that this channel coupling is critical. After these extensive checks, therefore, we believe that the present BSR-696 results are significantly more reliable than those from any previous theoretical work.

Figure 5 exhibits the cross section for electron impact ionization of carbon from the ^3P ground state. In large-scale pseudostate models, these results are obtained by adding the excitation cross sections for all pseudostates above the ionic ground state (the direct contribution) and an appropriate portion of the excitation cross sections of quasi-discrete states in the continuum. In our case, the latter include the $(2s2p^3)^1P^o$,$^1D^o$, and $^3S^o$ states. Of those, the $^1P^o$ and $^1D^o$ states have small excitation cross sections from the ground state and autoionize very quickly (for simplicity we will include their contribution in the direct signal), while the extent of the contribution from the $^3S^o$ state deserves special consideration.

The fully *ab initio* BSR results are in very good agreement with the semi-empirical BEB predictions of Kim and Desclaux [22]. The agreement with the experimental data of Brook *et al.* [23] is also good, although the theoretical results lie systematically below experiment. Looking at Fig. 1 of Kim and Desclaux [22], however, we see that their predictions (reproduced as the dash-dotted line in our figure) fall into almost perfect agreement with

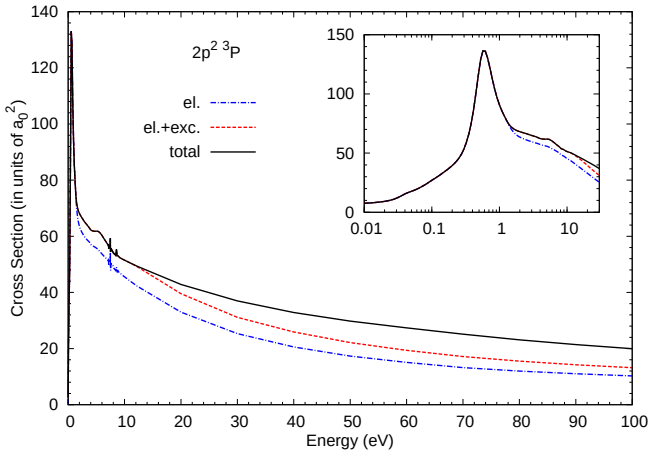

FIG. 6. (Color online) Angle-integrated elastic, elastic + excitation, and grand total (elastic + excitation + ionization) cross section for electron collisions with carbon in the $(2s^2 2p^2)^3 P$ ground state.

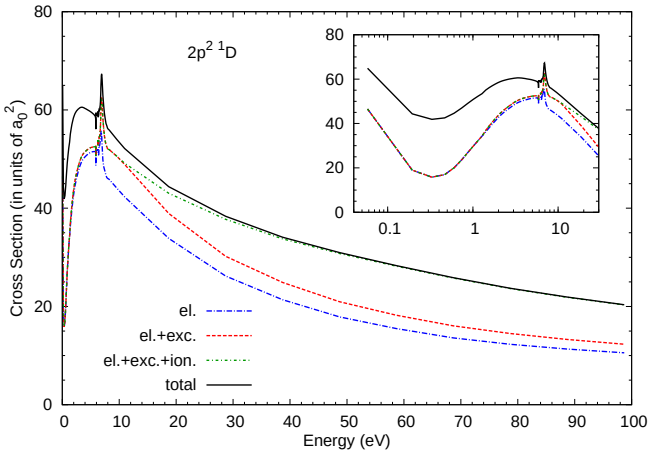

FIG. 7. (Color online) Angle-integrated elastic, elastic + excitation, elastic + excitation + ionization, and grand total cross section for electron collisions with carbon in the $(2s^2 2p^2)^1 D$ metastable state. In this case, the grand total cross section also contains deexcitation through superelastic scattering.

experiment — provided the cross section for excitation of the $(2s^2 2p^2)^3 P \rightarrow (2s2p^3)^3 S^o$ transition (see Fig. 2(f)) is added *entirely* to the direct ionization signal.

In spite of the success enjoyed by Kim's semiempirical approaches to both excitation [24] and ionization [25], however, the near-perfect agreement with experiment shown by Kim and Desclaux [22] appears to be accidental. As noted by the authors themselves, they were doubtful about the branching ratio between autoionization and optical decay, and they were using the optical oscillator strength from their own relatively small multi-configuration structure model, rather than the result obtained in a much larger bound-state close-coupling approach such as ours or that of Luo and Pradhan [18]. This difference, about a factor of about 2, directly enters into the BEB f-scaling [24] of the cross section for excitation of the $(2s2p^3)^3 S^o$ state (see Fig. 2(f)). A similarly large oscillator strength appeared in the calculation of Dunseath *et al.* [3] (see Tab. II of [2]), hence explaining the proximity between their results and those of BEB, especially at high energies.

Secondly, as discussed in subsection II A above, we estimate a branching ratio of 30% autoionization and 70% optical decay for the $(2s2p^3)^3 S^o$ state. Consequently, we added only 30% of our cross section for electron impact excitation of this state to estimate the total ionization cross section. The same was done with the results tabulated by Kim and Desclaux [22], even though their larger oscillator strength would shift the proportion further towards the optical decay.

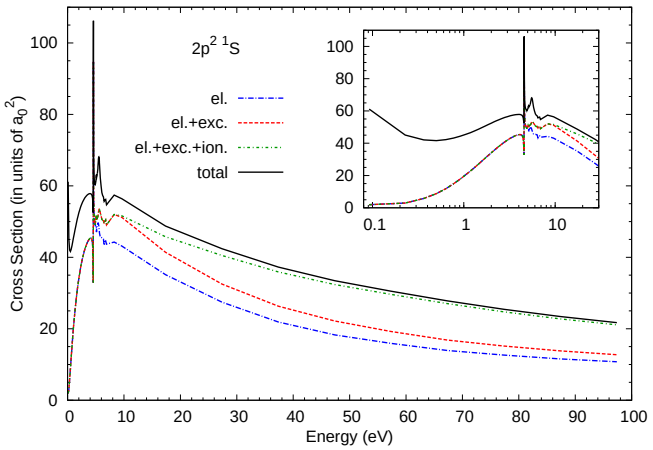

FIG. 8. (Color online) Angle-integrated elastic, elastic + excitation, elastic + excitation + ionization, and grand total cross sections for electron collisions with carbon in the $(2s^2 2p^2)^1 S$ metastable state. In this case, the grand total cross section also contains deexcitation through superelastic scattering.

C. Elastic, total excitation, ionization, and grand total cross sections from the ground and metastable states

Figures 6-8 show our present results in a form that might be useful for many plasma applications. Specifically, we show how the grand total cross section is composed of the elastic contribution, all inelastic excitation processes summed up, ionization, and – in the case of the excited metastable initial states $(2s^2 2p^2)^1 D$ and $(2s^2 2p^2)^1 S$ – *superelastic deexcitation*. As seen in the insets of Figs. 7 and 8, the latter process, in which the incident electron causes a transition in the target to a lower state and hence gains energy itself, can be the dominant

process in the low-energy regime. This would be important if there is a significant amount of metastable atoms in the system.

D. Finestructure-resolved results

Although carbon is a light atom, spin-dependent effects are known to be important at very low energies, corresponding for instance to low electron temperatures in cold regions of the interstellar medium [26]. In this case transitions between the three states $(2s^2 2p^2)^3P_{0,1,2}$ with different total electronic angular momentum J must be considered. This problem was already investigated a long time ago by Johnson *et al.* [4], who used a relatively simple polarized pseudostate model [27] (labeled RM-pol) for the target description. In order to examine the accuracy of their calculation, we performed a 314-state semirelativistic BSR calculation. Due to the march larger complexity associated with the intermediate coupling scheme, we were only able to include far fewer target continuum pseudostates in this BSR-314 model than in the BSR-696 non-relativistic calculation. Both expansions yield approximately the same number of scattering channels, leading to matrices of rank up to about 120,000 that can be handled with our current computational resources. The two models, nevertheless, still provide similar values for the ground state polarizabilities, namely $11.31\,a_0^3$ and $11.18\,a_0^3$, respectively, in BSR-696 and BSR-314. We noticed, however, a very slow convergence of the close-coupling expansion regarding the position of the low-energy structure (see below). Whereas the BSR-696 model provides a converged position of the $(2s2p^3)^2P$ resonance without any additions to the close-coupling expansion, we included separately optimized MCHF expansions for the $(2s2p^3)^2P_{1/2,3/2}$ resonances in the second part of Eq. (2) in the BSR-314 calculation to ensure the correct resonance positions. The same approach is usually employed in standard R-matrix calculations, including the work of Johnson *et al.* [4].

Figure 9 shows the results for elastic scattering between each of the finestructure states as well as for the inelastic $(2s^2 2p^2)^3P_0 \rightarrow (2s^2 2p^2)^3P_{1,2}$ and $(2s^2 2p^2)^3P_1 \rightarrow (2s^2 2p^2)^3P_2$ transitions. If there were no relativistic effects present at all, then the curves for the three elastic transitions would look identical. However, they are clearly different in both the early calculation and the current work. This is mainly due to the broad $(2s^2 2p^3)^2P_{1/2,3/2}$ resonances, as discussed by Johnson *et al.* [4]. Although the maximum of the cross section occurs around 0.6 eV, the resonance is apparently coupling to the finestructure levels (separated by merely 5 meV [17]) in significantly different ways. For example, the $^3P_0 - ^3P_0$ curve does not exhibit a maximum at all. Except for a slight shift of the maxima towards lower energies, the present results are in good agreement with the RM-pol predictions. For the low energies considered here, such an approach already appears to be sufficient. Hence we expect the BSR-314 results, which were generated with a much more extensive structure description, to be highly accurate in this energy range.

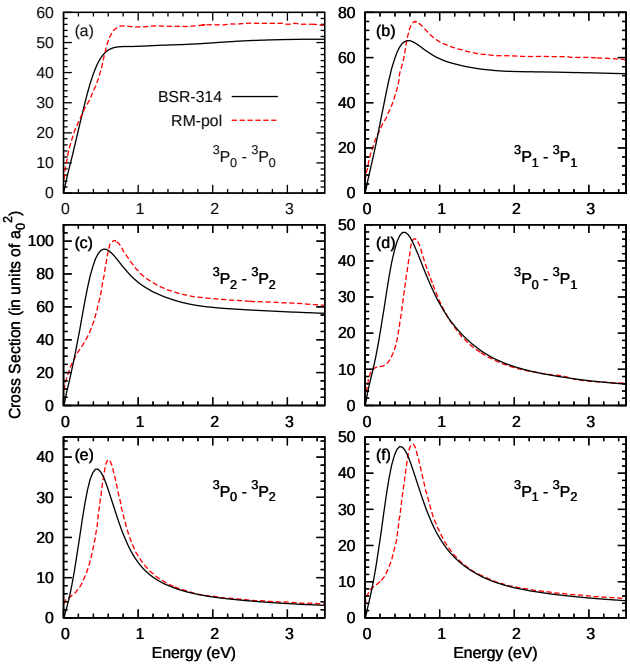

FIG. 9. (Color online) Finestructure-resolved cross sections for elastic scattering and electron-induced transitions between the $(2s^2 2p^2)^3P_{0,1,2}$ states. The present semirelativistic BSR-314 results are compared with those from a previous R-matrix calculation (RM-pol) by Johnson *et al.* [4].

IV. SUMMARY AND CONCLUSIONS

We have presented a revised set of cross sections for elastic scattering as well as electron-induced excitation, deexcitation, and ionization of carbon initially in its ground or metastable states. The calculations were performed with the B-spline R-matrix method, where a B-spline basis is employed for the representation of the continuum functions and the use of non-orthogonal orbital sets allows for high flexibility, and hence accuracy, in the construction of the target wavefunctions. The latter can be independently optimized for each state of interest.

Compared to our previous BSR calculation [2], the target description was further improved in the current work. Furthermore, a large number of pseudostates was included in the close-coupling expansion. These pseudostates allow for the treatment of two important features, namely: i) inclusion of the influence of coupling to the ionization continuum (and high-lying Rydberg states) on transitions between the discrete states that are most interesting for plasma modeling; and ii) *ab initio* calculations of the ionization cross section. In order to do the latter for this particular case of interest, an estimate for

the branching ratio between autoionization and optical decay of the metastable $(2s2p^3)^3S^o$ state was obtained as well.

Not surprisingly, the present results are significantly different from the previous BSR predictions, as well as those obtained by Dunseath *et al.* [3] who carried out a standard$R$-matrix calculations with the Belfast code [13]. Although the limited amount of data available in the literature (virtually none from beam experiments, except for the ionization data of Brook *et al.* [23]) does not allow for an unambiguous conclusion, our experience with such calculations leads us to suggest that the present results are the most accurate and hence should be used for modeling purposes as the preferred set of *ab initio* term-resolved data for this collision system. We plan to upload these results to the LXCat database in the near future. They are also available from the authors upon request.

ACKNOWLEDGMENTS

We thank Stuart Loch for pointing out the need for reliable data for the e−C collision system. This work was supported by the United States National Science Foundation under grants No. PHY-1068140 and No. PHY-1212450, and by the XSEDE allocation No. PHY-090031. Y.W. was sponsored by the China Scholarship Council and would like thank Drake University for their hospitality during his visit.

[1] http://www.lxcat.laplace.univ-tlse.fr/database.php
[2] O. Zatsarinny, K. Bartschat, L. Bandurina, and V. Gedeon, Phys. Rev. A **71** (2005) 042702.
[3] K. M. Dunseath, W. C. Fon, V. M. Burke, R. H. G. Reid, and C. J. Noble, J. Phys. B **30**, 277 (1997).
[4] C. T. Johnson, P. G. Burke, and A. E. Kingston, J. Phys. B **20** (1987) 2553.
[5] O. Zatsarinny and K. Bartschat, Phys. Rev. A **85** (2012) 062710.
[6] O. Zatsarinny and K. Bartschat, Phys. Rev. A **86** (2012) 022717.
[7] C. P. Ballance and D. C. Griffin, J. Phys. B **37** (2004) 2943.
[8] O. Zatsarinny, Comp. Phys. Commun. **174** (2006) 273.
[9] I. Bray and A. T. Stelbovics, Phys. Rev. A **46** (2002) 6995.
[10] K. Bartschat, E. T. Hudson, M. P. Scott, P. G. Burke, and V. M. Burke, J. Phys. B **29** (1996) 115.
[11] O. Zatsarinny and K. Bartschat, Phys. Rev. Lett. **107** (2011) 023203.
[12] O. Zatsarinny and K. Bartschat, Phys. Rev. A **85** (2012) 062709.
[13] K. A. Berrington, W. B. Eissner, and P. H. Norrington, Comput. Phys. Commun.**92** (1995) 290.
[14] N. R. Badnell (2012), http://amdpp.phys.strath.ac.uk/rmatrix/
[15] O. Zatsarinny and C. Froese Fischer, Comp. Phys. Commun. **180**, 2041 (2009).
[16] C. Froese Fischer, Comp. Phys. Commun. **176**, 559 (2007).
[17] Yu. Ralchenko *et al.* (2012), NIST Atomic Spectra Database (Version 5), http://physics.nist.gov/pml/data/asd.cfm
[18] D. Luo and A. K. Pradhan, J. Phys. B **22**, 3377 (1989).
[19] W. L. Wiese, J. R. Fuhr, and T. M. Deters, *Atomic Transition Probabilities of Carbon, Nitrogen and Oxygen: a Critical Data Compilation of NIST* (Washington, DC: American Chemical Society, 1996).
[20] P. G. Burke, *R-Matrix Theory of Atomic Collisions*, Springer-Verlag (Berlin, Heidelberg 2011)
[21] N. Badnell, J. Phys. B **32**, 5583 (1999); see also http://amdpp.phys.strath.ac.uk/UK_RmaX/codes.html
[22] Y.-K. Kim and J. P. Desclaux, Phys. Rev. A **66** (2002) 012708.
[23] E. Brook, M. F. A. Harrison, and A. C. H. Smith, J. Phys. B **11** (1978) 3115.
[24] Y.-K. Kim, Phys. Rev. A **64** (2001) 032713.
[25] Y.-K. Kim and M. E. Rudd, Phys. Rev. A **50 (1994)** 3954.
[26] L. Spitzer, *Physical Processes in the Interstellar Medium*, Wiley (New York, 1978).
[27] Vo Ky Lan, M. Le Dourneuf, and P. G. Burke, J. Phys. B **9** (1976) 1065.